Hyperelastic and Thermoreversible Iongels by Supramolecular PVA/Phenol Interactions

Gisela C. Luque[a], Matías L. Picchio[b], Ana P.S. Martins[c], Antonio Dominguez-Alfaro[c] Liliana C. Tomé[c], David Mecerreyes[c,d*] and Roque J. Minari[a,e*],

[a] Instituto de Desarrollo Tecnológico para la Industria Química (INTEC), CONICET, Güemes 3450, Santa Fe 3000, Argentina.

[b] Departamento de Química Orgánica, Facultad de Ciencias Químicas (Universidad Nacional de Córdoba), IPQA−CONICET, Haya de la Torre y Medina Allende, Córdoba 5000, Argentina.

[c] POLYMAT, University of the Basque Country UPV/EHU, Joxe Mari Korta Center, Avda. Tolosa 72, 20018 Donostia-San Sebastian, Spain.

[d] Ikerbasque, Basque Foundation for Science, 48013 Bilbao, Spain.

[e] Facultad de Ingeniería Química (Universidad Nacional del Litoral), Santiago del Estero 2829, Santa Fe 3000, Argentina.

*Corresponding authors:

David Mecerreyes (E-mail: david.mecerreyes@ehu.es)

Roque J. Minari (E-mail: rjminari@santafe-conicet.gov.ar)

ABSTRACT

Iongels have attracted much attention over the years as ion-conducting soft materials for applications in several technologies including stimuli-responsive drug release and flexible (bio)electronics. Nowadays, iongels with additional functionalities such as electronic conductivity, self-healing, thermo-responsiveness or biocompatibility are actively being searched for high demanding applications. In this work, we present a simple and rapid synthetic pathway to prepare hyperelastic and thermoreversible iongels. These iongels were prepared by supramolecular crosslinking between polyphenols biomolecules with a hydroxyl-rich biocompatible polymer such as poly(vinyl alcohol) (PVA) in the presence of ionic liquids. Using this strategy, a variety of iongels were obtained by combining different plant-derived polyphenol compounds such as gallic acid, pyrogallol, and tannic acid with imidazolium-based ionic liquids, namely [C_2mim][$N(CN)_2$] and [C_2mim][Br]. A suite of characterization tools was used to study the structural, morphological, mechanical, rheological and thermal properties of the supramolecular iongels. These iongels can withstand large deformations (40 % under compression) with full recovery, revealing reversible transitions from solid to liquid state between 87 to 125 °C. Finally, the polyphenol-based thermoreversible iongels shows appropriated properties for their potential application as printable electrolytes for bioelectronics.

TOC Graphic

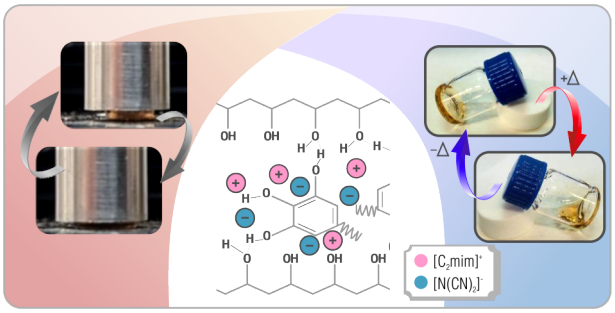

1. Introduction

Supramolecular materials have recently attracted considerable attention in different areas owing to their unique features such as self-healing, shape memory, and stimuli-responsiveness, among others.[1–6] In particular, supramolecular iongels are an emerging class of functional materials with exceptional properties for a vast assortment of applications.[7–11] These fascinating solid-state electrolytes consist of three-dimensional networks where gelling molecules self-assemble into nanometric structures through non-covalent inter-molecular interactions and the ionic liquid (IL) could act as structuring media during the gelation. Ionic liquids are low-melting-point salts with a unique combination of properties, namely non-volatility, thermal stability, high ionic conductivity, and wide electrochemical window.[12,13] The immobilization of ILs into supramolecular matrices allows to expand their application to all-solid devices such as electrochemical and biochemical sensors,[14] drug delivery systems,[15] batteries and supercapacitors,[16] fuel cells,[17] actuators,[18] or field-effect transistors. [19] Furthermore, the IL's features can be tuned by the choice of the anion-cation pair, which opens a huge number of possibilities to obtain materials with distinct properties, depending on the application requirements.

Dynamic supramolecular iongels are typically designed from low molecular weight gelators (LMWG)[20–23] or biopolymers, encompassing glycolipids, gelatin, carrageenans, guar gum, and cellulose,[24–28] providing materials with biomolecular functions (e.g. biocatalytic activity and biodegradability). However, this type of iongels frequently results in materials lacking the sturdiness required for many applications.[29,30] High mechanical robustness and dynamic properties (self-healing, thermoreversibility and shape-memory) seem to be features difficult to reach simultaneously in this type of materials. In particular, thermoreversible supramolecular iongels are scarcely found in the literature despite holding great potential for printed-bioelectronics applications.[31–34] Hence, there is a challenging need for creating new

supramolecular iongels combining thermoreversibility and stretchability, while preserving the unique ionic and conductivity properties given by the IL.

Currently, the bioelectronics area is looking for new soft-ionic systems to match biology and electronics.[35] Indeed, biobased iongels can be ideal candidates to prepare new advanced bioelectronics materials, owing to their well-known excellent properties as ion conductors and easily tailored physical-chemical features such as good elasticity toughness and adhesiveness. This combination of properties allows to reach performances that could not be achieved by conventional polymers. In this context, Leleux *et al*. proposed the preparation of iongels based on 1-ethyl-3-methylimidazolium ethyl sulfate ionic liquid within a poly(ethylene glycol) diacrylate network to be employed in long-term cutaneous recordings.[36] Isik and coworkers also investigated the preparation and the characterization of cholinium-based ion gels and their use as solid electrolytes in cutaneous electrophysiology.[37]

Despite the ability of polyphenols to form supramolecular interactions such as hydrogen bonding, metal-ligand coordination and π-π staking, they have not yet been deeply studied for the formation of iongels. [38,39] Herein, and to the best of our knowledge, we report for the first time that plant-derived phenolic molecules can assist the formation of thermoreversible and hyperelastic iongels. In this new type of conductive soft materials, polyphenol supramolecular chemistry is used to induce the gelation of a biocompatible hydroxyl-rich polymer, in the presence of imidazolium-based ILs. The polyphenols employed are pyrogallol-containing molecules ubiquitous in the plant kingdom with remarkable antioxidant, anti-inflammatory and antibacterial properties valuable for therapeutic bioelectronics.[40] Notably, only simple hot-dissolution and room temperature-cooling steps were needed to produce gelation; and this approach can be easily applicable to other desired ILs. Interestingly, strong polymer-gallol complexes led to networks with near-covalent elastic moduli, while having phase transition temperatures suitable for printing applications.[41] Coupled with

the use of different phenolic compounds, a plethora of solid-state electrolytes can be rationally built, as well a vast array of material properties can be reached through the implementation of this strategy.

2. Experimental section

2.1. Materials

Poly(vinyl alcohol) (PVA, Merck, degree of hydrolysis 99%, Mw 145 kDa), gallic acid (GA, Merck, ≥99.0%), pyrogallol (PGA, Carlo Erba, ACS reagent), tannic acid (TA, Biopack, ACS reagent), 1-ethyl-3-methylimidazolium bromide ([C_2mim][Br], IoLiTec), 1-ethyl-3-methylimidazolium dicyanamide ([C_2mim][$N(CN)_2$]), abcr 98%) were used as supplied. Distilled-deionized water was used for all experiments.

2.2 Preparation of iongels

In a typical experiment to prepare iongels with 10% of polymer concentration and GA, 0.05 g of PVA was dissolved in 0.5 g of water as solvent under vigorous stirring at 90 °C. Then the 0.5 g of IL, and 0.0239 g GA were added. After complete dissolution of all components, the mixed solution was poured into silicone moulds and left at room temperature until gelation. In all cases, a molar ratio of PhC's functional groups/PVA's hydroxyl groups of 0.5 was used. The polymer concentration was fixed at 10 or 20 wt% in relation to the IL amount. The same procedure was applied for the synthesis of others iongels based on PGA or TA.

2.3 FTIR spectroscopy

Total Reflection Fourier Transform Infrared Spectroscopy (ATR-FTIR) of the iongels were collected using a Bruker ALPHA spectrometer from 400 to 4000 cm^{-1}. The resolution was 4 cm^{-1} after 24 scans.

2.4 Rheological Behavior

The measurements were performed in an Anton Paar Physica MCR 301 rheometer. The gel-sol transition temperature ($T_{gel\text{-}sol}$) of the supramolecular iongels was investigated by dynamic mechanical thermal analysis (DMTA) using a parallel-plate geometry (8 mm in diameter). The whole temperature studied ranged from 20 to 90 °C with a heating rate of 2 °C min^{-1}. All the experiments were conducted at 1 Hz and 0.1% of strain.

2.5 Thermal Analysis

Thermal properties of materials were analyzed by thermogravimetric analysis (TGA) and differential scanning calorimetry (DSC). For TGA analysis, a TA instruments Q500 equipment was used. Samples of 10 mg were heated from 25 to 250 °C with a heating rate of 10 °C.min^{-1}, under nitrogen atmosphere. The temperature at maximal decomposition rate (T_{max}) was determined as the temperature at main peak of the derivative weight loss curve.

DSC experiments were performed on a Perkin Elmer 8500 DSC equipped with an Intracooler III. Samples (ca. 3 mg) were crimped in non-recyclable aluminum hermetic pans and analyzed under nitrogen atmosphere by heating and cooling cycles at a rate of 20 °C min^{-1}. First, the samples were heated from 25 to 150 °C and kept isothermally for 3 min to erase thermal history. Subsequently, the samples were cooled down to -70 °C and kept isothermal for 10 min. Second run heating cycles were conducted and used to further investigate the phase transition behavior of all samples.

2.6 X-Ray Diffraction

The crystalline structure of the samples was examined by X-Ray Diffraction (XRD) using a Shimadzu XD-D1 equipment with a Cu Kα radiation source, between 5° to 60° with a scan rate of 2°C min^{-1}.

2.7 Compression

The elastic behavior of the iongels was studied using a universal testing machine (INSTRON 3344) at 23 ºC and 55% of relative humidity. All samples, of around 1 mm of thickness, were subjected to a compression test, in which a 10 mm diameter plane-tip is moved down at a constant speed (1 mm/min), until compressing samples 40 % their height.

2.8 Scanning Electron Microscopy

Scanning Electron Microscopy (SEM) measurements were performed on JEOL JSM-6490LV at 5kV. The freeze-drying samples with different compositions were sliced transversely. Then, frontal and transversal samples were mounted onto an aluminum holder with double-sided carbon tape. Subsequently, the holder was homogenized at vacuum pressure overnight. Afterwards, the samples were sputter-coated with gold (Alto 1000, Gatan Inc.). Finally, the morphology of the different samples was studied at different magnifications.

3. Results and Discussion

Iongels were prepared by supramolecular crosslinking between polyphenols biomolecules with a hydroxyl-rich biocompatible polymer such as poly(vinyl alcohol) (PVA) in the presence of ionic liquids. The gel nature of these materials is given by the supramolecular interactions, which take place between PVA and PhC via hydrogen bonding dynamically crosslinking the ionic liquids. The effect of the polymer concentration and chemical structure of the PhC on the iongels properties was explored. The PhC's GA, PGA and TA were selected as physical crosslinkers, due to their similar structure but distinctive number or type of functional groups, offering the opportunity to control the supramolecular interactions with PVA chains. The $[C_2mim][Br]$ and $[C_2mim][N(CN)_2]$ were the ILs employed. Moreover, the $[C_2mim][Ac]$ IL was further tested in the iongels preparation, but it was found that gelation does not occur in the presence of this ionic liquid. Although further studies are needed, we hypothesize that

this behavior is due to esterification reactions that might involve the imidazolium cation and PhC to yield methyl-sustituted molecules, which hinder the gel formation.[42] For this purpose, two PVAs with different degrees of hydrolysis were studied, 87% and 99%, aiming to control the polymer/phenol supramolecular interactions. Only iongels prepared from fully hydrolyzed PVA (99%) are here discussed, because those with partially hydrolyzed PVA (87%) resulted in mechanically weak materials.

A schematic representation of the iongel supramolecular assembly is shown in Figure 1 A. In all cases, free-standing and elastic iongels were obtained (Figure 1B). Interestingly, most of the supramolecular iongels were dark solids, except that prepared with [C_2mim][Br], TA, and GA. We hypothesized that this distinctive appearance is related to the well known formation of ortho-quinone species as a consequence of the redox couples IL/PhC or PhC oxidation. It is also worth mentioning that high amounts of PVA (20 wt%) cannot be solubilized in the presence of the multifunctional TA and [C_2mim][Br], avoiding the iongel formation at this high polymer loading.

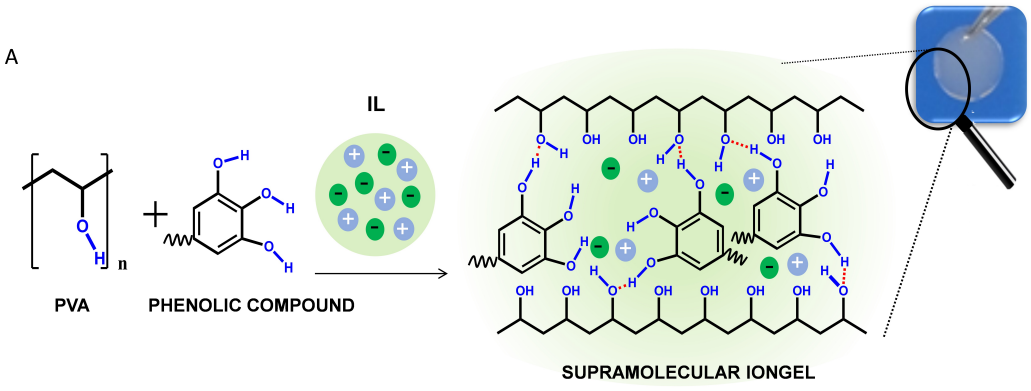

Figure 1. (A) Schematic representation of the supramolecular iongel formation. (B) Pictures of all the prepared supramolecular iongels.

The nature of the chemical interactions in the supramolecular iongels was investigated by Total Reflection Fourier Transform Infrared Spectroscopy (ATTR-FTIR) analysis. Figure 2 shows the FTIR spectra of PVA, GA, $[C_2mim][N(CN)_2]$ and PVA-GA-$[C_2mim][N(CN)_2]$ iongel. The characteristic peaks of each neat component were identified in the iongel spectrum. A wide absorption band at 3014–3680 cm^{-1} was attributed to the stretching vibration of OH groups of PVA and GA; two bands at 2931 and 2853 cm^{-1} were assigned to the asymmetrical and symmetrical stretching of CH groups, respectively. Two bands at 1426 and 1085 cm^{-1} can be assigned to the in-plane O–H bending and C–OH stretching of PVA, respectively.[43] The C=O and C–OH stretching bands corresponding to GA can be seen at 1662 and 1309 cm^{-1}, respectively. The stretching corresponding to C≡N of the IL dicyanimide anion[44] can also be observed at 2250 cm^{-1} in the iongel spectrum. As it can be seen in Figure 2, the vibrational modes corresponding to the main groups of neat PVA and $[C_2mim][N(CN)_2]$ were not modified after the gel formation process (Figure 2). Contrary to what was reported regarding the formation of supramolecular PVA-GA hydrogels,[43] no significant shifts were observed in the C=O stretching band and phenyl C–OH stretching corresponding to GA for the iongels prepared in the present work. This is probably attributed to the high IL content in the iongel formulation, which can overlap the visualization of peaks shifting in the iongel formed through multiple hydrogen-bonding interactions.

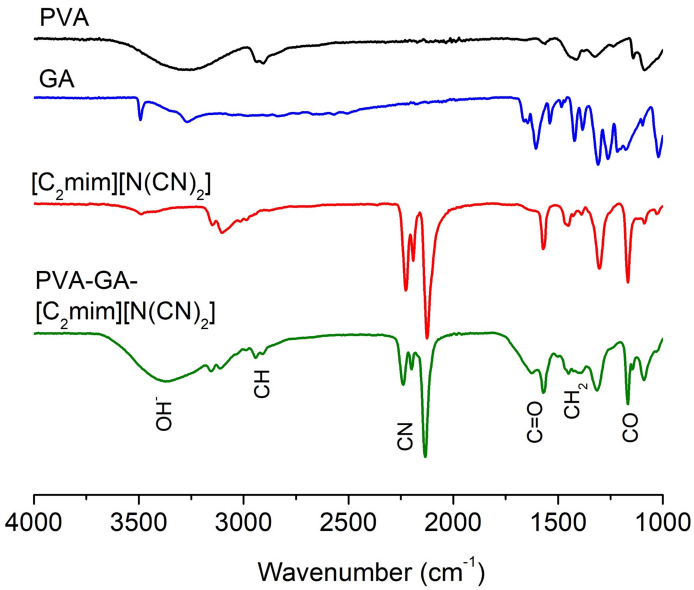

Figure 2. FTIR spectra of PVA, GA, $[C_2mim][N(CN)_2]$ and PVA-GA-$[C_2mim][N(CN)_2]$ iongel with 10 % polymer concentration (PVA and GA).

In order to evaluate the gel-sol transition of the prepared iongels, their viscoelastic behavior *versus* temperature was investigated by dynamic mechanical thermal analysis (DMTA). Figure 3 shows the results for PVA-TA-$[C_2mim][Br]$ iongel with 10 wt% polymer concentration, while the thermomechanical evolution of the obtained iongel materials with both ILs and different PhC's is plotted in Figure S1. Polyphenol-based iongels displayed a solid-like behavior at low temperature, which is shown by an elastic modulus (G′) that is higher than the viscous modulus (G″). As the temperature increased, a transition from an elastic network to a viscoelastic liquid (G″ > G′) occurred. This transition temperature from an elastic network to the liquid state ($T_{gel\text{-}sol}$) was defined as the temperature at which G′ = G″ upon heating. Moreover, and comparing the systems with the same polymer concentration and IL, no significant effects regarding the different PhC chemical structures were observed on the iongels $T_{gel\text{-}sol}$ (see Figure S1). Interestingly, it was found that an increase in PVA concentration up to 20 wt% led to higher $T_{gel\text{-}sol}$ of the iongels, probably due to the formation of a higher number of effective hydrogen bonding interactions in the material (see Table S1 of the SI). For instance, in the systems containing $[C_2mim][Br]$, the $T_{gel\text{-}sol}$ varied

between 87 and 110 °C, respectively, when the polymer concentration increased from 10 to 20 wt%. All the prepared supramolecular iongels showed reversible gel-sol phase transitions (see Figure 3B and video S1 of the SI), a key requirement for their potential application as printable soft materials in bioelectronics.

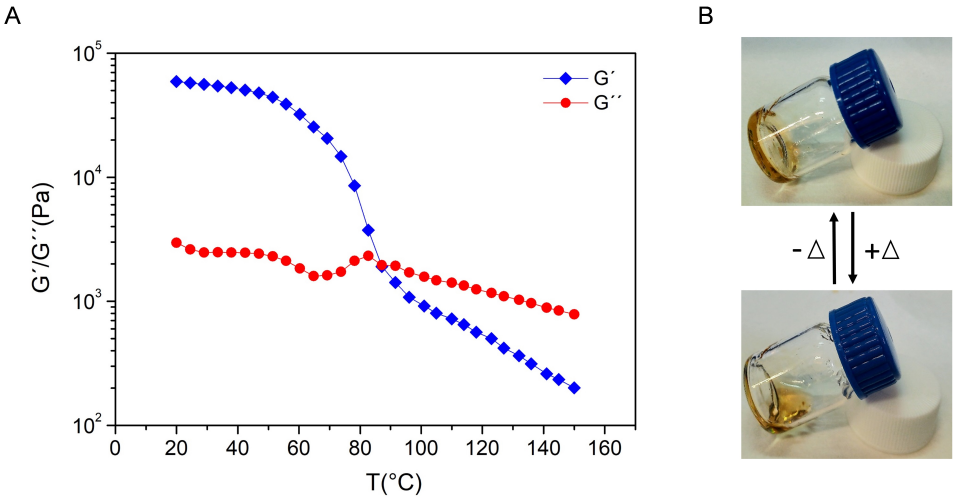

Figure 3. (A) Thermomechanical behavior of the PVA-TA-[C_2mim][Br] supramolecular iongel. (B) Schematic picture of the reversible gel-sol phase transition of PVA-TA-[C_2mim][$N(CN)_2$] iongel. The iongel polymer concentration was 10 wt%.

The thermal properties of the iongels were also analyzed by thermogravimetric analysis (TGA) and differential scanning calorimetry (DSC). The TGA results (Figure 4) showed that the iongels present good thermal stability, with maximum decomposition temperatures (T_{max}) ranging from 290 to 310°C. In addition, the TGA analysis revealed lower decomposition temperatures (at 50% of weight loss, $T_{50\%}$) for the iongels containing [C_2mim][Br] than those of the [C_2mim][$N(CN)_2$]. This is in agreement with the degradation profile of the neat ILs.

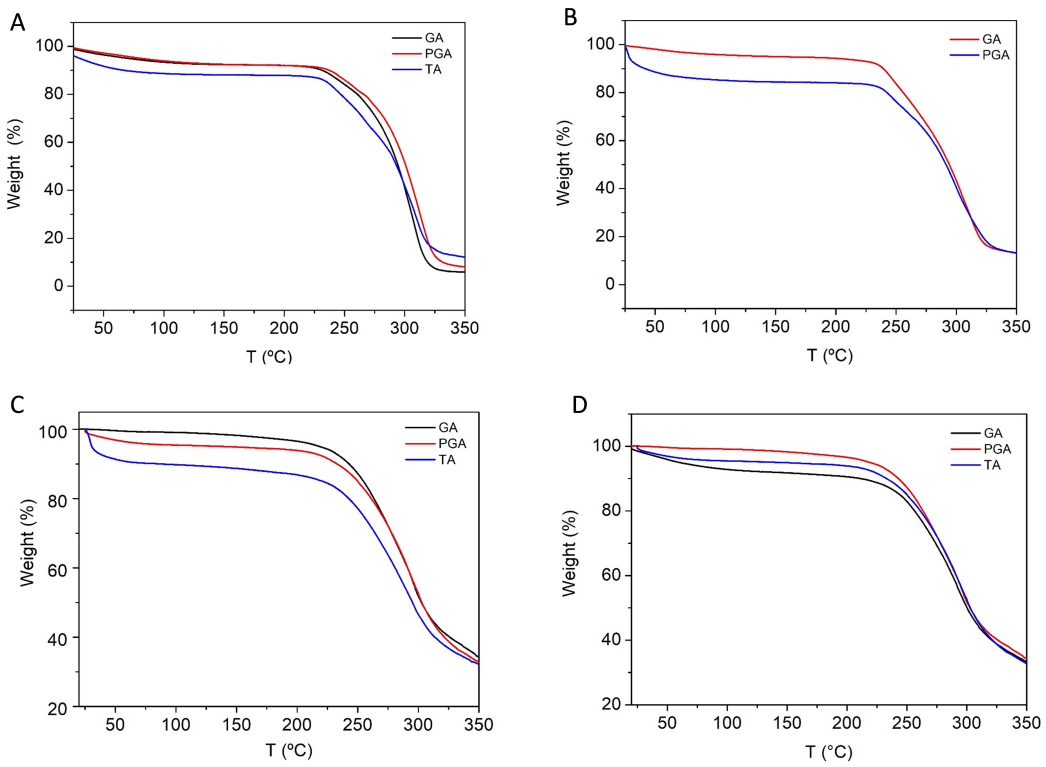

Figure 4. TGA analysis of PVA-PhC-[C_2mim][Br] (A,B) and PVA-PhC-[C_2mim][$N(CN)_2$] (C,D). The iongels polymer concentrations were 10 wt% (A,C) and 20 wt% (B,D).

Furthermore, DSC analysis was performed in order to investigate the thermal transitions of the supramolecular iongels (Figure 5). For instance, an outstanding decrease in the glass transition temperature (T_g) from 37 to -47 °C was observed for the PVA-GA-[C_2mim][Br] iongel. This behavior can be attributed to the entrapped water and IL into the iongel, which has a powerful plasticizing effect, indicating an overall increase of polymer chain mobility.[45–47] However, when using the [C_2mim][$N(CN)_2$] IL, T_g values were not detected in the whole temperature range studied, probably due to limitations concerning the lowest temperature operation (-70 ºC) of the DSC equipment used in this work.

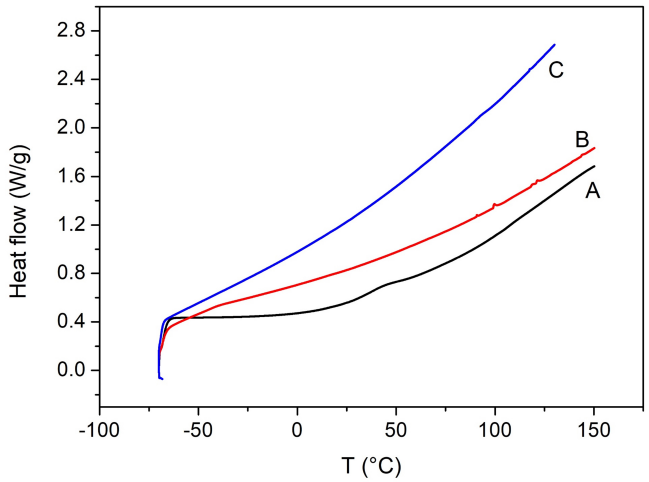

Figure 5. DSC thermograms of PVA A), PVA-GA-[C_2mim][Br] B), and PVA-GA-[C_2mim][$N(CN)_2$] C). The iongels polymer concentration was 10 wt%.

The microstructure of the iongels was studied by X-ray diffraction (XRD). It is known that PVA chains can be organized into crystalline phases through freezing-thawing cycles.[48,49] Our recent results showed that phenolic compounds can induce the organization of PVA chains within hydrogels in semi-crystalline domains with a spatial arrangement completely different than that of the neat PVA.[43] For this reason, it was important to investigate the diffraction pattern of the prepared iongels in order to get insights regarding the IL effect on the PVA/phenol supramolecular assembly. From Figure S2, it can be observed that the supramolecular iongels showed a characteristic XRD spectrum of an amorphous material, suggesting that the ILs are playing an important role in the supramolecular interactions, preventing to some extent the organization of the typical PVA/phenol arrangement previously observed in hydrogels.

From the DMTA results showed in Figure 3, it can be seen that the iongels behave at room temperature as solid-like materials with a predominant elastic modulus. These observations are limited at small deformation (0.1 %). To give more insight about the elastic behavior of the supramolecular iongels, the axial compression at large deformation, that is 40%, of iongels were investigated. Assuming that iongels are

incompressible (their volume remain constant during the test), a compression deformation of 40 % represents a large expansion (around 130 %) in their diameter.

In the absence of IL, the PVA-GA hydrogel was a fragile material, easily tearable upon handling (see video S2 of the SI), while the prepared iongels present hyperelastic behavior. They are able to resist large deformations, recovering their initial shape after load remove with a non-linear evolution of compression stress *versus* strain (Figure 6.A and video S3 and S4 of the SI). Figure S3 of SI illustrates two consecutive cycles of compression for PVA-TA-[C_2mim][Br] iongel, where the material instantaneous capability to recovery after each compression cycle is demonstrated. Moreover, Figure 6(B) displays the Young modulus (*E*) obtained for the prepared supramolecular iongel, which was calculated in the limit at low strain. When increasing the polymer concentration into the iongel, an increase in the *E* modulus was observed, which is a consequence of the higher dynamic intermolecular interactions formed. The use of TA, a highest functional polyphenol, in PVA-TA-[C_2mim][$N(CN)_2$] iongels with a polymer concentration of 20% showed the highest modulus, 3.5×10^4 Pa, one magnitude order greater than that of GA-based iongel (1×10^3 Pa). Curiously, when using the [C_2mim][Br] IL, no significant differences were observed on E values for TA and GA based iongels.

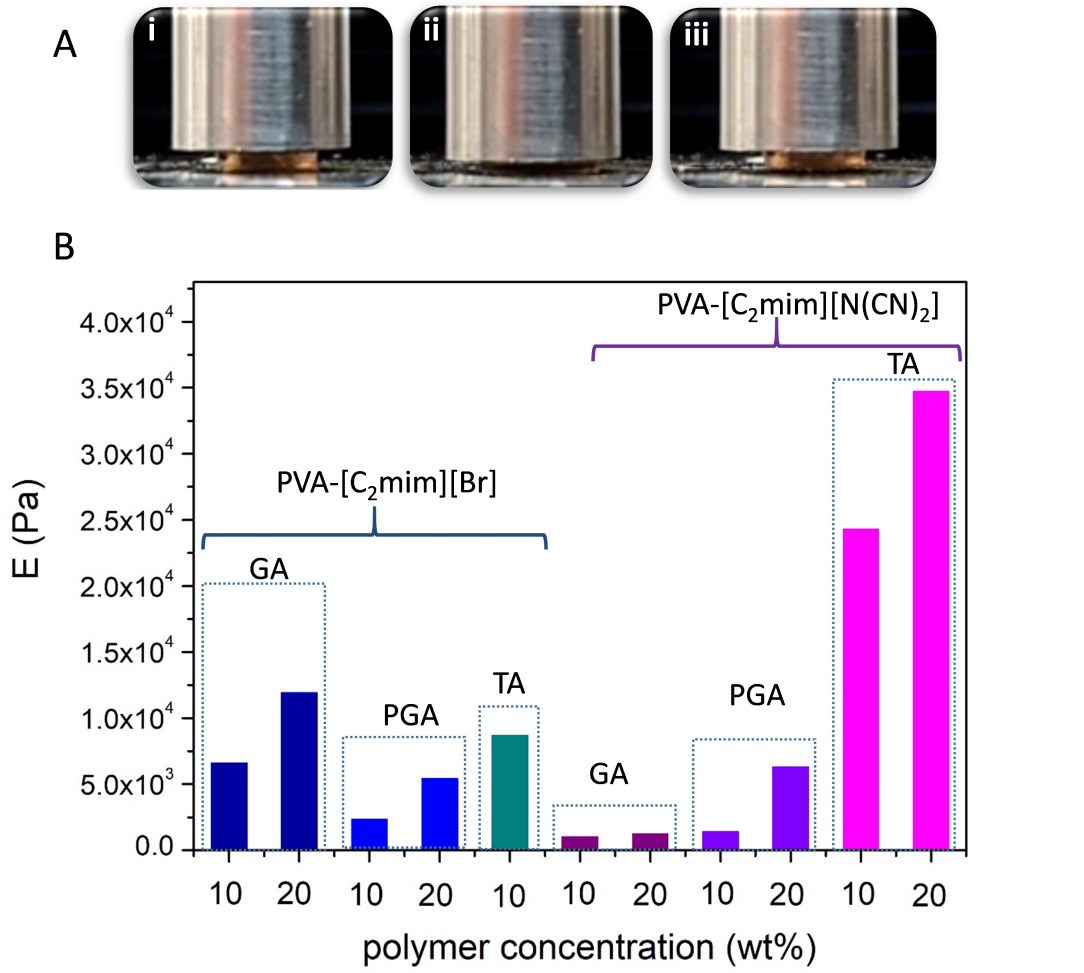

Figure 6. (A) Pictures of compression test sequence: (i) initial state, (ii) full compressed, and (iii) elastic recovery. (B) Compression modulus for the supramolecular iongels.

With the intent of reveal the different microstructurations of PVA/phenol arrangement in presence of different ILs, SEM micrographs of the PVA-GA supramolecular iongels surface are shown in Figure 7 (A, B). The PVA-GA-[C_2mim][Br] and PVA-GA-[C_2mim][N(CN)] iongels present notably distinctive surface morphologies. When using the [C_2mim][Br] IL, a dense and homogeneous structure with the presence of microcrystals can be observed (Figure 7 A). We hypothesized that these microdomains can probably be attributed to a possible crystallization of the [C_2mim][Br] IL, upon water evaporation, since the melting temperature of this IL is around 81 °C. On the other hand, PVA-GA-[C_2mim][$N(CN)_2$] iongel (Figure 7 B) display a less dense structure with

even roughness, meaning that the [C_2mim][$N(CN)_2$] is certainly better homogeneously dispersed in the polymer matrix. Also, for comparison purposes, the SEM images (cross-sectional cut of freeze-drying samples) of the PVA-GA-[C_2mim][Br] iongel and the PVA-GA hydrogel previously reported[43] are given in Figure 7 (C,D), respectively. The SEM cross-section micrograph of the PVA-GA-[C_2mim][Br] iongel reveals that this iongel has a lower dense porous structure (Figure 7C) compared to that of the PVA-GA hydrogel previously prepared without IL. In fact, in the absence of IL, the PVA-GA hydrogel shows irregular porous walls (Figure 7 D). These poorly interconnected globules degraded its mechanical properties, as above mentioned. Conversely, the iongel showed good structural interconnection, resulting in outstanding mechanical robustness and elasticity when compared to that of the hydrogel material. We believe that this bulk-connectivity is reached mainly due to the presence of the IL that can act as a structuring media during the gel formation process.

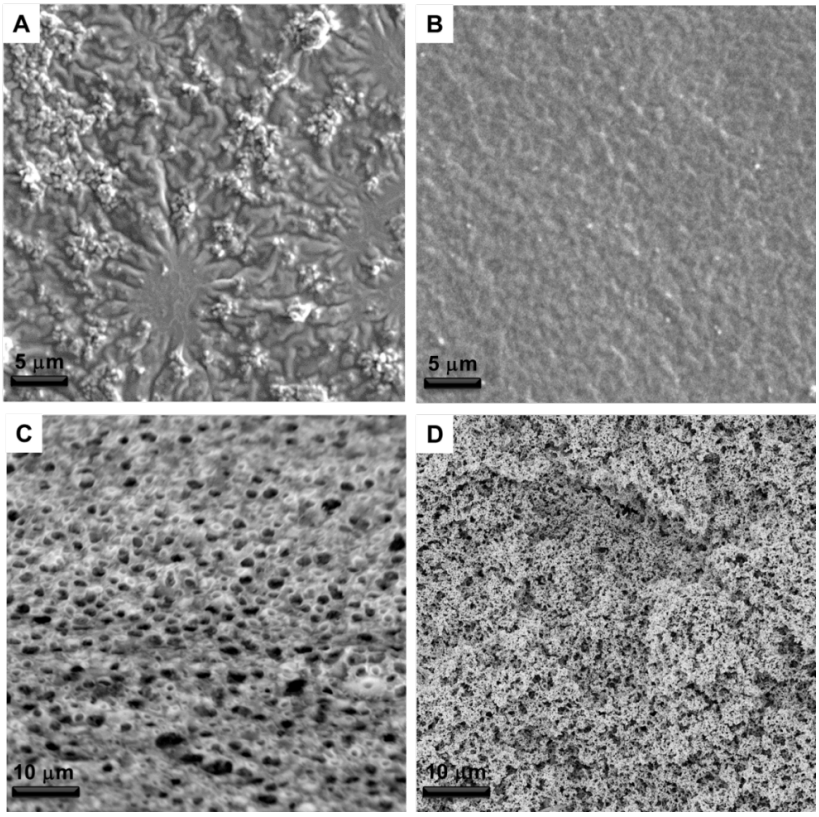

Figure 7. SEM images of iongels surface: A) PVA-GA-[C_2mim][Br], and B) PVA-GA-[C_2mim][$N(CN)_2$]. Internal morphologies of freeze-drying PVA-GA-[C_2mim][Br] iongel C) and PVA-GA hydrogel D). The iongels polymer concentration was 10 wt%.

4. Conclusions

This work proposes a novel method to prepare hyperelastic and dynamic supramolecular iongels consisted of a biocompatible polymer (PVA) and three different plat-derived phenolic compounds. The bore ILs in these iongels are based on the $[C_2mim]^+$ cation and either $[Br]^-$ or $[N_{(CN)2}]^-$ anions. The different ILs lead to iongels with diverse morphological and mechanical properties. For instance, the use of $[C_2mim][Br]$ IL resulted in iongels with a dense and homogeneous structure with the presence of microcrystals (SEM), higher young modulus (6,7 kPa) and lower $T_{gel\text{-}sol}$ (87 °C) compared to those of the iongel containing the $[C_2mim][N(CN)_2]$ IL (1 kPa and 105 °C). The formation of the supramolecular iongels are based on hydrogen bonding interactions between PVA and the polyphenol, resulting in thermoreversible iongels with suitable transition temperatures (between 87 and 110 °C) for printing applications. Moreover, the supramolecular iongels are flexible and can withstand large elastic deformations with full recovery. In sum, the thermoreversible iongels proposed in this work unveil excellent properties and potential to be employed in bioelectronics.

Acknowledgment

This work was supported by Marie Sklodowska-Curie Research and Innovation Staff Exchanges (RISE) under the grant agreement No 823989 “IONBIKE”. Also, the financial support received from CONICET, UNL, and ANPCyT (all of Argentina) is gratefully acknowledged. Liliana C. Tomé has received funding from the European Union’s Horizon 2020 research and innovation programme under the Marie Sklodowska-Curie grant agreement no. 745734.

References

[1] J. L. Mann, A. C. Yu, G. Agmon, E. A. Appel, *Biomater. Sci.* **2018**, *6*, 10.

[2] X. Yan, F. Wang, B. Zheng, F. Huang, *Chem. Soc. Rev.* **2012**, *41*, 6042.

[3] S. S. Hou, Y. Y. Hsu, J. H. Lin, J. S. Jan, *ACS Macro Lett.* **2016**, *5*, 1201.

[4] G. Zhang, Y. Chen, Y. Deng, T. Ngai, C. Wang, *ACS Macro Lett.* **2017**, *6*, 641.

[5] K. Kawamoto, S. C. Grindy, J. Liu, N. Holten-Andersen, J. A. Johnson, *ACS Macro Lett.* **2015**, *4*, 458.

[6] R. Dong, Y. Pang, Y. Su, X. Zhu, *Biomater. Sci.* **2015**, *3*, 937.

[7] I. Del Agua, D.Mantione, N. Casado, A. Sanchez-Sanchez, G.G. Malliaras, D. Mecerreyes, *ACS Macro Lett.* **2017**, *6*, 473.

[8] J. Le Bideau, L. Viau, A. Vioux, *Chem. Soc. Rev.* **2011**, *40*, 907.

[9] P. C. Marr, A. C. Marr, *Green Chem.* **2015**, *18*, 105.

[10] S. Chen, N. Zhang, B. Zheng, B. Zhang, J. Song, *ACS Appl. Mater. Interfaces* **2018**, *10*, 44706.

[11] P. Guo, A. Su, Y. Wei, X. Liu, Y. Li, F. Guo, Jian Li, Z. Hu, J. Sun, *ACS Appl. Mater. Interfaces* **2019**, *11*, 19413.

[12] M. P. Singh, R. K. Singh, S. Chandra, *Prog. Mater. Sci.* **2014**, *64*, 73.

[13] N. Chen, H. Zhang, L. Li, R. Chen, S. Guo, *Adv. Energy Mater.* **2018**, *8*.

[14] D. Khodagholy, V.F. Curto, K.J. Fraser, M. Gurfinkel, R. Byrne, D. Diamond, G.G. Malliaras, F. Benito-Lopez, R.M. Owens, *J. Mater. Chem.* **2012**, *22*, 4440.

[15] L. Viau, C. Tourné-Péteilh, J. M. Devoisselle, A. Vioux, *Chem. Commun.* **2010**, *46*, 228.

[16] A. S. Shaplov, R. Marcilla, D. Mecerreyes, *Electrochim. Acta* **2015**, *175*, 18.

[17] M. Díaz, A. Ortiz, M. Isik, D. Mecerreyes, I. Ortiz, *Int. J. Hydrogen Energy* **2014**,

40, 11294.

[18] S. Imaizumi, H. Kokubo, M. Watanabe, *Macromolecules* **2012**, *45*, 401.

[19] C. Müller, M. Hamedi, R. Karlsson, R. Jansson, R. Marcilla, M. Hedhammar, *Adv. Mater.* **2011**, *23*, 898.

[20] A. Wu, F. Lu, P. Sun, X. Qiao, X. Gao, L. Zheng, *Langmuir* **2017**, *33*, 13982.

[21] S. Chen, B. Zhang, N. Zhang, F. Ge, B. Zhang, X. Wang, J. Song, *ACS Appl. Mater. Interfaces* **2018**, *10*, 5871.

[22] R. Ranjan, K. Rawat, H. B. Bohidar, *Phys. Chem. Chem. Phys.* **2017**, *19*, 22934.

[23] T. Zhou, X. Gao, F. Lu, N. Sun, L. Zheng, *New J. Chem.* **2016**, *40*, 1169.

[24] G. Singh, G. Singh, K. Damarla, P.K. Sharma, A. Kumar, T.S. Kang *ACS Sustain. Chem. Eng.* **2017**, *5*, 6568.

[25] T. J. Trivedi, K. S. Rao, A. Kumar, *Green Chem.* **2014**, *16*, 320.

[26] P. Vidinha, N.M.T. Lourenço, C. Pinheiro, A. R. Brás, T. Carvalho, T. Santos-Silva, A. Mukhopadhyay, M. J. Romão, J. Parola, M. Dionisio, J. M. S Cabral, C. A. M Afonso, S. Barreiros, *Chem. Commun.* **2008**, 5842.

[27] C. J. Smith, D.V. Wagle, H. M. O'Neill, B.R. Evans, S.N. Baker, G.A. Baker, *ACS Appl. Mater. Interfaces* **2017**, *9*, 38042.

[28] B. Zhang, G. Sudre, G. Quintard, A. Serghei, L. David, J. Bernard, E. Fleury, A. Charlot, *Carbohydr. Polym.* **2017**, *157*, 586.

[29] K. Prasad, D. Mondal, M. Sharma, M.G. Freire, C. Mukesh, J. Bhatt, *Carbohydr. Polym.* **2018**, *180*, 328.

[30] A. Sharma, K. Rawat, P. R. Solanki, H. B. Bohidar, *Int. J. Biol. Macromol.* **2017**, *95*, 603.

[31] Y. He, T. P. Lodge, *Macromolecules* **2008**, *41*, 167.

[32] A. Noro, Y. Matsushita, T. P. Lodge, *Macromolecules* **2008**, *41*, 5839.

[33] C. C. Hall, C. Zhou, S. P. O. Danielsen, T. P. Lodge, *Macromolecules* **2016**, *49*, 2298.

[34] J. C. Ribot, C. Guerrero-Sanchez, R. Hoogenboom, U. S. Schubert, *Chem. Commun.* **2010**, *46*, 6971.

[35] S. M. Kim, N. Kim, Y. Kim, M. S. Baik, M. Yoo, D. Kim, W. J. Lee, D. H. Kang, S. Kim, K. Lee, M. H. Yoon, *NPG Asia Mater.* **2018**, *10*, 255.

[36] P. Leleux, C. Johnson, X. Strakosas, J. Rivnay, T. Hervé, R.M. Owens, G.G. Malliaras, *Adv. Healthc. Mater.* **2014**, *3*, 1377.

[37] M. Isik, T. Lonjaret, H. Sardon, R. Marcilla, T. Herve, G.G. Malliaras, E. Ismailova, D. Mecerreyes, *J. Mater. Chem. C* **2015**, *3*, 8942.

[38] J. Shim, K.Y. Bae, H.J. Kim, J.H. Lee, D.G. Kim, W.Y. Yoon, J.C. Lee, *ChemSusChem* **2015**, *8*, 4133.

[39] Z. Li, J. Wang, R. Hu, C. Lv, J. Zheng, *Macromol. Rapid Commun.* **2019**, *40*, 1800776.

[40] P. Diaz, S. C. Jeong, S. Lee, C. Khoo, S. R. Koyyalamudi, *Chinese Med.* **2012**, *7*, 12361.

[41] K. H. Lee, S. Zhang, Y. Gu, T. P. Lodge, C. D. Frisbie, *ACS Appl. Mater. Interfaces* **2013**, *5*, 9522.

[42] A. T. Tran, P.H. Lam, A.M. Miller, D.J. Walczyk, J. Tomlin, T.D. Vaden, L. Yu *RSC Adv.* **2017**, *7*, 18333.

[43] E. M. Euti, A. Wolfel, M.L. Picchio, M.R. Romero, M. Martinelli, R.J. Minari, C. Igarzabal, *Macromol. Rapid Commun.* **2019**, *40*, 1900217.

[44] K. Periyapperuma, C. Pozo-Gonzalo, D. R. Macfarlane, M. Forsyth, P. C. Howlett, *ACS Appl. Energy Mater.* **2018**, *1*, 4580.

[45] R. Atakan A. Bical, E. Celebi, G. Ozcan, N. Soydan, A.S. Sarac, *J. Ind. Text.* **2019**, *49*, 141.

[46] N. H. A. M. Hashim, R. H. Y. Subban, *AIP Conf. Proc.* **2018**, *2031,* 020021.

[47] I. J. Shamsudin, A. Ahmad, N. H. Hassan, H. Kaddami, *Solid State Ionics* **2015**, *278*, 11.

[48] S. R. Stauffer, N. A. Peppast, *Polymer* **1992**, *33*, 3932.

[49] J. Tavakoli, J. Gascooke, N. Xie, B. Z. Tang, Y. Tang, *ACS Appl. Polym. Mater.* **2019**, *1*, 1390.